



HAL
open science

Thermal performance of a building envelope including microencapsulated phase change materials (PCMs): A multiscale experimental and numerical investigation

Franck Komi Gbekou, Rahma Belloum, Nawal Chennouf, Boudjemaa Agoudjil, Abderrahim Boudenne, Karim Benzarti

► To cite this version:

Franck Komi Gbekou, Rahma Belloum, Nawal Chennouf, Boudjemaa Agoudjil, Abderrahim Boudenne, et al.. Thermal performance of a building envelope including microencapsulated phase change materials (PCMs): A multiscale experimental and numerical investigation. *Building and Environment*, 2024, 253, pp.111294. 10.1016/j.buildenv.2024.111294 . hal-04468826

HAL Id: hal-04468826

<https://enpc.hal.science/hal-04468826v1>

Submitted on 26 Feb 2024

HAL is a multi-disciplinary open access archive for the deposit and dissemination of scientific research documents, whether they are published or not. The documents may come from teaching and research institutions in France or abroad, or from public or private research centers.

L'archive ouverte pluridisciplinaire **HAL**, est destinée au dépôt et à la diffusion de documents scientifiques de niveau recherche, publiés ou non, émanant des établissements d'enseignement et de recherche français ou étrangers, des laboratoires publics ou privés.

1 **Thermal performance of a building envelope including microencapsulated**
2 **phase change materials (PCMs): A multiscale experimental and numerical**
3 **investigation**

4 Franck Komi Gbekou¹, Rahma Belloum², Nawal Chennouf², Boudjemaa Agoudjil^{2*},
5 Abderrahim Boudenne^{3*}, Karim Benzarti¹

6 ¹Laboratoire Navier, Université Gustave Eiffel, Ecole Nationale des Ponts et Chaussées
7 (ENPC), Centre National de la Recherche Scientifique (CNRS), F-77447 Marne la Vallée,
8 France.

9 ²Laboratoire de Physique Energétique Appliquée (LPEA), Université Batna-1, Les Allées 19
10 Mai, Route de Biskra, Batna, Algérie

11 ³Centre d'Études et de Recherche en Thermique, Environnement et Systèmes (CERTES),
12 Université Paris-Est Créteil, France.

13 **Abstract**

14 This study aims to assess the thermal behavior of a cement mortar (denoted M15D) incorpo-
15 rating microencapsulated biobased phase change materials at both wall and building scales. A
16 bi-climatic chamber setup was employed to subject the wall to distinct thermal conditions
17 simulating outdoor and indoor environments, using heating and cooling solicitations. Tempera-
18 ture sensors, strategically positioned at various depths, allowed the monitoring of tempera-
19 ture within the walls during the experiments.

20 On a building scale, the thermal performance of M15D was predicted using two mathematical
21 models describing heat transmission in porous systems incorporating phase-change materials.
22 Numerical simulations were carried out using COMSOL Multiphysics and EnergyPlus soft-
23 ware. The results obtained were validated against experimental data, at wall scales.

24 The outcomes highlighted that the incorporation of microencapsulated biobased phase change
25 materials significantly influences both building energy consumption and interior temperature.
26 The heat storage capacity offered by M15D demonstrated a significant impact on thermal per-
27 formance, leading to energy savings of up to 33% for heating and 31% for cooling, contingent
28 on climate conditions. In conclusion, the integration of biobased phase change materials in the
29 cement mortar (M15D) display benefits in enhancing thermal performance at building scales.

30 **Keywords:** phase change materials (mPCM), experimental setups, energy saving, numerical
31 model.

32 ***Corresponding author:**

33 Pr. Boudjemaa Agoudjil, email :boudjemaa.agoudjil@univ-batna.dz

- 1 Laboratoire de Physique Energétique Appliquée (LPEA), Université Batna-1, Les Allées 19
- 2 Mai Route de Biskra, Batna, Algérie.

1 **1. Introduction**

2 Global warming and resource depletion have become central topics in the news, and current
3 trends indicate that we are approaching a crucial decision point. Population growth and over-
4 consumption are contributing to increased energy consumption and CO₂ emissions[1]. Ac-
5 cording to the Intergovernmental Panel on Climate Change (IPCC) in its latest 2023 report,
6 global surface temperatures have already risen by 1.1°C compared to the pre-industrial period,
7 and this is projected to increase to 1.5°C by 2030. Furthermore, the 2022 Global Status Report
8 for Buildings and Construction, published by the UN Environment Program, reveals that CO₂
9 emissions from building use reached approximately 10 gigatons in 2022 [2]. One of the most
10 resource-intensive industries is the construction sector, responsible for 36% of global energy
11 consumption. Energy consumption in buildings encompasses the entire energy usage, from
12 raw materials to the final building, with a significant portion dedicated to maintaining com-
13 comfortable living conditions within structures. For instance, in France, heating alone accounts for
14 approximately 65% of energy consumption in the residential sector and 43% in the tertiary
15 sector [3].

16 To overcome the rising trend of energy consumption and global warming, it is crucial to offer
17 alternative solutions to the public while promoting eco-friendly options. There is an urgent
18 need to develop innovative solutions that enhance thermal efficiency in buildings [1, 4]. Nu-
19 merous research efforts are currently underway to develop new building materials aimed at
20 improving their thermophysical properties for energy-efficient and environmentally friendly
21 construction alternatives [5-8]. One such solution is passive thermal energy storage systems
22 (TES), which enable the storage of a certain amount of energy for later use with minimal en-
23 ergy loss between storage and release [8]. Among thermal energy storage systems, latent heat
24 thermal energy storage is particularly well-suited for building applications[9-12]. This tech-
25 nology relies on the use of phase change materials (PCMs), which are materials that undergo
26 a change in their physical state (transitioning from solid to liquid and vice versa) in response
27 to temperature fluctuations, thereby storing and releasing energy during these phase transi-
28 tions[13, 14]. Combining PCMs with building materials such as concrete or mortar holds
29 great promise as it enhances the thermal properties of these materials and provides energy
30 storage capabilities. Studies on PCM walls in building applications have demonstrated signif-
31 icant benefits. For example, Bahrar et al. [15] reported a reduction of up to 1.7°C in the max-
32 imum temperature recorded when using an additional PCM panel. Al-Absi et al. [16] in their
33 investigation of the addition of a PCM panel to concrete in a test box, observed temperature
34 reductions of up to 6°C compared to the reference box as outdoor temperatures increased. Li
35 et al.[10], reported a dampening effect on indoor/outdoor temperature differences in a room
36 equipped with a multi-layer system of cementitious walls incorporating an insulating PCM
37 layer, resulting in energy savings of up to 30%.

38 The rapid advancements in alternative building materials research have spurred the develop-
39 ment of simulation tools aimed at analyzing the performance of these materials under differ-
40 ent sizes and environmental conditions [13, 14]. These simulation tools rely on mathematical

1 models to depict heat flow within building materials, enabling them to forecast temperature
2 patterns. Nevertheless, given the extensive range of materials, PCM (Phase Change Material)
3 combinations, and integration techniques accessible for building envelopes, optimizing PCM
4 usage necessitates a comprehensive assessment of factors such as building construction, PCM
5 integration methods, and their specific placement within the structure [17, 18].

6 Several techniques exist for incorporating PCMs into construction materials, facilitating their
7 integration into a wide range of building components [7]. The current methods employed in-
8 clude direct embedding, immersion, form-stable and shape-stabilization, as well as micro,
9 macro, and nano encapsulation [7, 19, 20]. In this paper, we focus on the microencapsulation
10 of PCMs, a process where the PCM is encapsulated within microcapsules ranging from 1 μm
11 to 1 mm in diameter. This method involves enclosing a small quantity of PCM within another
12 substance, such as a lipid, polymer, or inorganic component, to create microcapsules that act
13 as a protective barrier between the PCM and its surrounding environment. The resulting mi-
14 crocapsules can then be incorporated into various materials, such as mortar or concrete, to
15 form composite materials with enhanced thermal properties.

16 Numerous tools are currently available for simulating building energy consumption, such as
17 BLAST, BSim, DeST, DOE, ECOTECT, Ener-Win, Energy Express, Energy-10, EnergyPlus,
18 eQUEST, IDA-ICE, IES, HAP, HEED, PowerDomus, SUNREL, Tas, TRACE, and
19 TRNSYS. For our work, we chose the EnergyPlus tool due to its robust validation and ability
20 to interface with various systems like HVAC and renewable energy [21].

21 Indeed, despite a good understanding of the physical equations governing PCM behavior,
22 there is a scarcity of numerical models available for its simulation. Most existing numerical
23 models tend to focus on whole-building modeling, using unidirectional heat transmission
24 through walls and an equation for the air energy balance to determine the typical room air
25 temperature [22-24]. However, adapting these models to various building arrangements can
26 be complex.

27 To comprehensively harness the potential of PCM energy storage when integrated with
28 HVAC systems, such as natural night ventilation during the summer, the adoption of a modu-
29 lar simulation tool structure becomes imperative. This approach would substantially enhance
30 the optimization and analysis of PCM performance. In fact, one notable effort in simulating
31 PCM walls has been presented by Ibáñez et al. [23] using EnergyPlus. Their method adopts a
32 global energetic perspective, taking temperatures (both wall and air) as inputs and generating
33 data for the active layer as outputs. This approach enables the assessment of PCM's impact on
34 the overall energy balance within a room. However, further experimental confirmations are
35 still needed to validate and enhance the accuracy of this approach.

36 In the existing literature, the studies have predominantly investigated the effect of incorporat-
37 ing an additional PCM panel within multi-layered insulation systems. Furthermore, to our
38 knowledge, very little research has been conducted on the thermal performance of a homoge-

1 neous cement mortar system that integrates microencapsulated PCM distributed throughout its
2 thickness. This study aims to fill this research gap by thoroughly investigating a homogeneous
3 mortar wall that incorporates bio-based PCM. The wall will be subjected to various thermal
4 conditions, and its thermal performance will be systematically compared to that of a reference
5 mortar wall. To facilitate this research, a custom-made experimental setup was constructed to
6 replicate a bi-climatic environment. This setup exposes each surface of the wall to distinct
7 hygrothermal conditions, simulating both indoor and outdoor environments. The incorpora-
8 tion of hygrothermal sensors at various depths within the wall has enabled the recording of
9 temperature variations throughout its thickness.

10 The primary objective of this research is to improve the heat consumption efficiency of build-
11 ings by enhancing their thermo-physical characteristics and developing composite walls with
12 bio-based microencapsulated phase change material incorporated into mortar. The study em-
13 ploys an enthalpy approach and COMSOL analysis to create an unsteady thermal transport
14 numerical model of bio-based PCM. This model helps to understand the mechanism of heat
15 storage and temperature regulation of PCM within the wall. Moreover, numerical simulations
16 are performed to investigate thermal inertia and energy savings.

17 The fundamental idea behind this research starts with the experimental characterization of the
18 bio-based PCM at both material and wall scales. The collected data are then used to validate
19 the numerical model developed using COMSOL-Multiphysics, which enables the calculation
20 of the bio-based PCM enthalpy as a function of temperature. Subsequently, this validated
21 model will be integrated into EnergyPlus to provide comprehensive results representing the
22 performance of the bio-based PCM at the building scale under real climatic conditions, con-
23 sidering aspects like thermal inertia and energy consumption. The goal is to assess the thermal
24 performance and energy-saving potential of the bio-based PCM when incorporated into build-
25 ing envelopes.

26 **2. Materials and experimental methods**

27 **2.1 Materials**

28 Two cement mortar walls were studied in this work: a reference cement mortar wall (noted
29 M0) and a wall made from the reference mortar with the addition of microencapsulated bio-
30 based phase change materials (M15D). The reference mortar is a pre-existing formulation de-
31 signed for additive manufacturing [25]. It comprises an ordinary Portland cement
32 EXTREMAT® CEM I 52.5 N (denoted OPC), a fast-setting sulfo-aluminous cement (denoted
33 CSA), both products by the VICAT company (L'Isle-d'Abeau, France), a superplasticizer
34 VISCOCRETE TEMPO 11 (SP) water reducer from SIKA (Baar, Switzerland), and standard-
35 ized sand with a maximum particle size of 2mm, provided by Société Nouvelle du Littoral
36 (Leucate, France).

37 A commercial bio-based PCM was selected for the study. It's denoted CrodaTherm™
38 ME29D and is in the aqueous dispersion form of microencapsulated particles in water (solid

1 content of about 50 wt.%). The particles are an organic PCM core (from plant-based
 2 feedstocks) surrounded by a formaldehyde-free acrylic polymer shell. The PCM has a melting
 3 and crystallization point of 29°C and 24°C, respectively, and heats of fusion and crystalliza-
 4 tion of 183 kJ/kg and 179 kJ/kg, according to the supplier's technical datasheet [26].

5 In a material-scale study on the effect of the addition of these PCMs on the mechanical and
 6 thermophysical properties of the mortar, we have prepared and tested various mortars with
 7 PCM content up to 13.5 wt.%. We have shown the beneficial effect of the addition of PCMs
 8 on the thermophysical properties of mortars while reducing mechanical performance. A sig-
 9 nificant improvement in the thermophysical properties is found with the reduction of the
 10 thermal conductivity by 72% ($0.6 \text{ W.m}^{-1} \cdot \text{K}^{-1}$ compared to $2.3 \text{ W.m}^{-1} \cdot \text{K}^{-1}$ for M0) with 11
 11 wt.% of PCMs added. This formulation is denoted M15D and was then chosen to conduct a
 12 comparative study at the wall scale to compare the thermal responses of a wall made with
 13 mortar to the ones of the reference mortar. The composition of the two mortars (M0 and
 14 M15D) is displayed in Table 1.

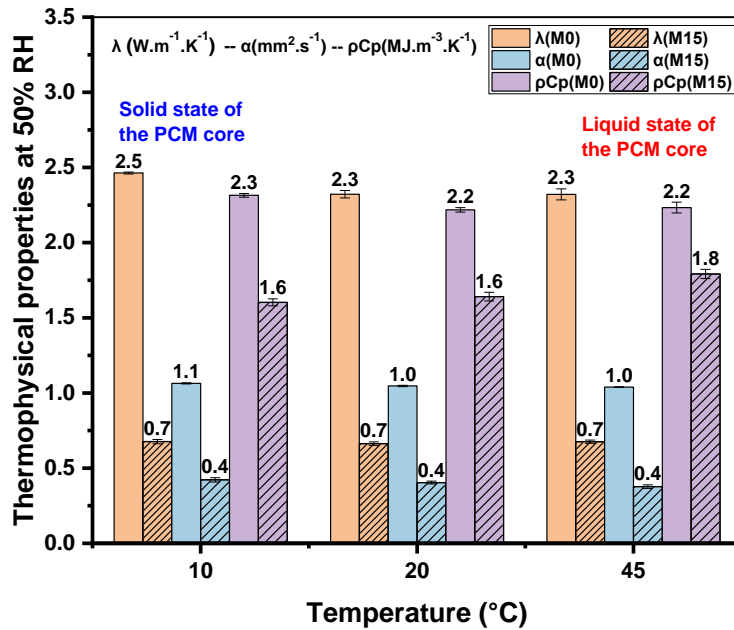
15 **Table 1.** Composition of the two mortar formulations used in this work.

Type of mortar	Sand (g)	OPC (g)	CSA (g)	SP (g)	Mass of mPCM particles (g)	Total water (g)	W/C ratio	Weight fraction of mPCM particles (%)	Volume fraction of mPCM particles (%)
M0	1350	1059	80	3	-	399	0.4	0	0
M15D	1350	1059	80	3	433	1006	0.9	11	21

16

17 2.2 Thermophysical properties

18 Several measurements were conducted to determine the thermophysical properties of the two
 19 mortars. For this purpose, the Hot Disk method (HD) was employed, using a TPS 2500 S de-
 20 vice with a sensor "Kapton ref 5501" having a radius of 6.4 mm. The HD method allows for
 21 the simultaneous measurement of thermal conductivity (λ in $\text{W.m}^{-1} \cdot \text{K}^{-1}$), thermal diffusivity (α
 22 in $\text{m}^2 \cdot \text{s}^{-1}$), and volumetric heat capacity ($\rho \cdot C_p$ in $\text{MJ.m}^{-3} \cdot \text{K}^{-1}$). Several measurements were
 23 conducted in a controlled moisture environment of 50% RH and a temperature range from
 24 10°C to 45°C, covering all states of the core of the phase change material.



1

2 **Figure 1.** Thermophysical properties (at 50% RH) of M0 and M15 were determined by the
 3 HD method (solid and liquid states of the PCM core).

4 The thermophysical properties of the reference (M0) and bio-based PCM mortar (M15D) are
 5 presented in **Figure 1** as a function of temperature variation, with error bars indicating stand-
 6 ard deviations based on five measurements for each temperature. The M15D mortar exhibits
 7 significantly lower values for all three measured properties compared to the reference materi-
 8 al, regardless of the temperature considered. For instance, at 20°C, the thermal conductivity of
 9 M15D is reduced by approximately 72%, dropping from 2.32 W.m⁻¹.K⁻¹ (for M0) to 0.68
 10 W.m⁻¹.K⁻¹. This decrease can be attributed to the low thermal conductivity of the bio-based
 11 PCM itself, which typically ranges from 0.25 to 0.35 W.m⁻¹.K⁻¹ depending on the physical
 12 state of the PCM core [27]. Additionally, the significant increase in porosity of the mortar
 13 containing bio-based PCM promotes thermal transfer through convection in the pores rather
 14 than through thermal conduction [21-23]. These findings agree with the observations of pre-
 15 vious studies by Dehdezi et al. [21], Hunger et al. [22], and Jayalath et al. [23], where the ad-
 16 dition of 5 wt.% PCMs into cement composites resulted in respective decreases in thermal
 17 conductivity of approximately 36%, 38%, and 45% compared to reference specimens.

18 2.3 Experimental setup of bi-climatic test cell

19 2.3.1 Preparation and instrumentation of walls

20 The studied test walls have a dimension of 50 × 50 × 10 cm³ and were prepared according to a
 21 mixing protocol displayed in our previous work. The walls were prepared and underwent sev-

1 eral months of curing in a laboratory environment at 20°C and under ambient humidity condi-
2 tions.

3 To record the hygrothermal response of the wall, temperature sensors were installed within
4 the walls. Each wall is equipped with a total of five sensors. One on the external faces and
5 three in the thickness. Three holes of 8mm in diameter were carefully drilled into the wall's
6 thickness at a depth of 25 cm. They are positioned at 2.5 cm, 5 cm, and 7.5 cm, respectively,
7 from the outer surface (Figure 2.a). The holes are spaced 15 cm apart vertically to prevent any
8 interference during the measurements. For precision of sensor position, the holes were per-
9 formed using a precision's column drilling machine.

10 2.3.2 *The bi-climatic experimental setup*

11 A homemade experimental setup was constructed to simulate a dual-climate environment for
12 a building. This setup involves the application of two different hygrothermal conditions on
13 opposite sides of the wall, simulating indoor and outdoor environmental conditions.

14 The system consists of a metallic frame built around a climatic chamber (Memmert ICH 260)
15 to connect the wall to both environments (indoor and outdoor). The indoor environment is a
16 laboratory room where the temperature is regulated at 20°C using an air conditioner. The rela-
17 tive humidity of the room is recorded over several weeks of measurements (between 45% and
18 55% RH) but is left uncontrolled to provide a daily-use impression.

19

20 To avoid thermal leaks, an expanded polystyrene (6 cm) is placed between the wall and the
21 frame. The insulation material is recovered with an insulating and vapor-barrier adhesive plas-
22 tic film. Therefore, hygrothermal exchanges may happen only in the central open area of
23 40'45 cm² (Figure 2.b). To ensure unidirectional (1D) hygrothermal transfer, all lateral sur-
24 faces were insulated using expanded polystyrene, allowing hygrothermal exchange exclusiv-
25 ily through the two exposed surfaces. Two additional sensors were positioned within the cli-
26 matic chamber and the laboratory room to record the indoor and outdoor temperature condi-
27 tions instantly. The insulation of the total setup is checked using a thermal infrared camera to
28 prevent heat loss and have a uniform transfer across the observed surface (Figure 2.c).

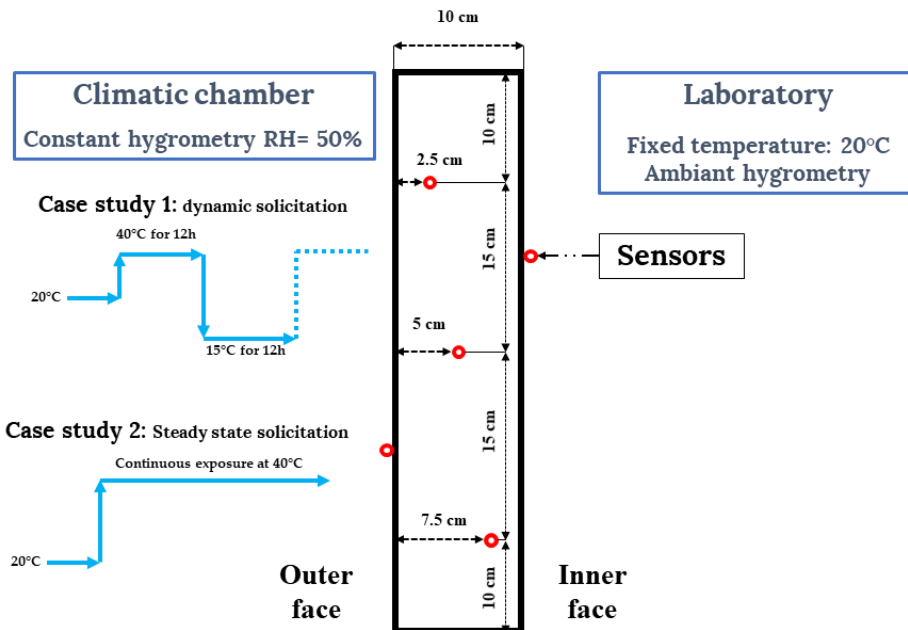


1
2 **Figure 2.** (a) Wall preparation with sensors; (b) Experimental setup; (c) IR image of the wall
3 to check uniform heat transfer and prevent heat losses.

4 **2.3.3 Experimental hygrothermal case study**

5 After the setup was performed, the two faces of the wall were stabilized at 20°C and 50% RH
6 for approximately one week, until all recorded measurements indicated the set point. Two
7 experimental programs were applied to each wall (Figure 3). The indoor environment is kept
8 constant during the two scenarios. It is set at 20°C with ambient humidity. The outdoor ther-
9 mal conditions are applied at a fixed humidity of 50% RH. These programs consist of:

- 10 • A day/night simulation involves varying temperatures between a heating (40°C) and a
11 cooling (15°C) phase, each lasting 12 hours.
12 • continuous heating at 40°C until reaching a steady-state condition.



13

1 **Figure 3.** Case studies applied to the wall.

2 **3. Mathematical model**

3 The existence of PCMs in three different states (solid, liquid, and solid-liquid coexistence)
4 adds complexity to the phase change heat transfer problem [18]. As latent heat is stored and
5 released over time, the interface between the two phases moves, making the simulation more
6 challenging.

7 To simplify the complex heat transfer process in mixing mortar and encapsulated PCM, the
8 following hypotheses are suggested to develop the analytical model [28]:

- 9 - Heat transfer is assumed to occur only in the thickness direction since it always
10 takes place between the inner and outer surfaces, leading to one-dimensional heat
11 transfer.
- 12 - Natural convection during the melting process of PCM and the undercooling effect
13 during the solidification process of PCM are neglected.
- 14 - The physical properties of other solid materials are considered constant.
- 15 - The PCM in the phase-change layer is assumed to be homogeneous and isotropic.
- 16 - The thermal contact resistance between layers is considered negligible.
- 17 - The liquid state of the PCM is assumed to be an incompressible Newtonian fluid,
18 following Fourier's heat conduction.

19 By applying these hypotheses, the analytical model aims to achieve simulation results while
20 reducing the complexities involved in the heat transfer process between mixing mortar and
21 encapsulated PCM.

22 According to the literature, there are two commonly used numerical methods for modeling
23 phase change materials (PCMs): the enthalpy method and the effective heat capacity method.
24 For this study, we have chosen to utilize the enthalpy method, which considers the liquid
25 state, solid state, and transition phase in PCM using the mixtures law.

26 To conduct a comprehensive investigation at both the wall scale and the building scale, we
27 employed two different software tools: COMSOL and EnergyPlus. However, the enthalpy
28 model is not readily available in both tools. To overcome this limitation, we utilized the flexi-
29 bility of COMSOL, which allows us to introduce the enthalpy model and then create a ready-
30 to-use function for EnergyPlus.

31 The enthalpy model [8, 29, 30] relies on enthalpy and temperature as dependent variables.
32 The advantage of this model is that it does not require the consideration of movement and
33 changes in the transition interface, allowing for the establishment of unified equations in all
34 three states of PCM (solid, liquid, and transition). Where, the enthalpy model is expressed as:

$$\rho \frac{dh}{dt} = \nabla(k \nabla T) \quad (1)$$

1 The total enthalpy (h) is the sum of the sensible and latent heats of the PCM and is related to
 2 the temperature of the PCM as follows:

$$h = \begin{cases} C_{PS}(T - T_m) + C_{PL}(T_m - T_a) - \theta \left(1 - \frac{T_a - T_m}{T_a - T} \right) - (C_{PS} - C_{PL}) \times (T_a - T_m) \times \ln\left(\frac{T_a - T}{T_a - T_m}\right) & T \leq T_m \\ C_{PL}(T - T_a) & T > T_m \end{cases} \quad (2)$$

3 where:

4 ρ : Density, ($kg.m^{-3}$)

5 λ : Thermal conductivity, ($W.m^{-1}.K^{-1}$)

6 C_{PS} : Specific heat capacity of solid state, ($J.kg^{-1}.K^{-1}$)

7 C_{PL} : Specific heat capacity of liquid state, ($J.kg^{-1}.K^{-1}$)

8 θ : Liquid fraction

9 T_m : Melting temperature ($23^\circ C$).

10 T_a : The end of the non-isothermal melting ($28^\circ C$).

11 The enthalpy-temperature function of the M15D was determined using COMSOL
 12 Multiphysics software, which can solve the unsteady heat transfer problem by the finite ele-
 13 ment method. The model is supplied by the properties presented in Table 2. The values of
 14 thermal capacity in solid and liquid states are obtained using the mixing law according to the
 15 results of Gbekou et al. [31]

16 **Table 2.** Thermal proprieties of M15 introduced in COMSOL-Multiphysics [31].

Properties	Density (kg/m^3)	Thermal capacity solid ($j/kg. k$)	Thermal capacity Liquid ($j/kg. k$)	Thermal conduc- tivity ($W/m. k$)
M15	1710	1026	1073	0.7

17 The results obtained using COMSOL for the enthalpy temperature relationship of M15, as
 18 shown in **Figure 4**, are incorporated into EnergyPlus to feed the PCM model. EnergyPlus,
 19 developed by the United States Department of Energy (US DOE), is widely used for whole-
 20 building energy simulations, and it offers the capability to model PCMs using a Conduction
 21 Finite Difference (CondFD) solution algorithm. The CondFD algorithm discretizes the layers
 22 of the building envelope into different nodes and numerically solves the heat transfer equa-
 23 tions using a finite difference method (FDM). In this study, the Fully Implicit Finite Differ-
 24 ence Scheme, coupled with an enthalpy temperature function to account for the phase change

1 energy, was adopted [32]. The following equations represent the method of the fully implicit
 2 schema used in EnergyPlus:

$$c_p \rho \Delta x \frac{T_i^{j+1} - T_i^j}{\Delta t} = k_w \frac{T_i^{j+1} - T_i^{j+1}}{\Delta x} + k_E \frac{T_{i+1}^{j+1} - T_i^{j+1}}{\Delta x} \quad (3)$$

3 With:

$$k_w = \frac{k_{i+1}^{j+1} + k_i^{j+1}}{2} \quad (4)$$

4

$$k_E = \frac{k_{i-1}^{j+1} + k_i^{j+1}}{2} \quad (5)$$

5

$$C_p^*(T) = \frac{h_i^j - h_i^{j-1}}{T_i^j - T_i^{j-1}} \quad (6)$$

6 Where:

7 $k_i = k(T_i^{j+1})$: if thermal conductivity is variable.

8 T: Temperature

9 Cp: Specific heat capacity, (J/(kg·K))

10 i: Node being modeled

11 i+1: Adjacent node to interior of construction

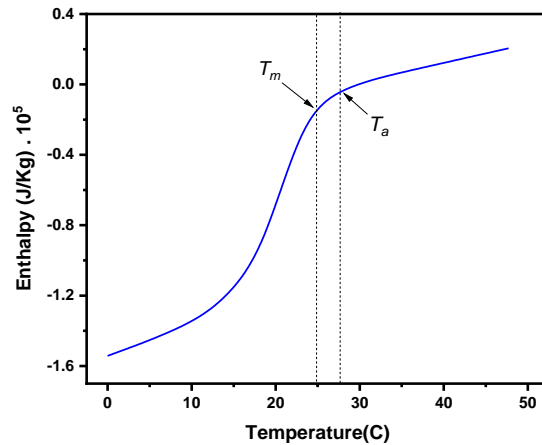
12 i-1: Adjacent node to exterior of construction

13 j+1: New time step

14 j: Previous time step

15 Δt : Time step

16 Δx : Finite difference layer thickness



1

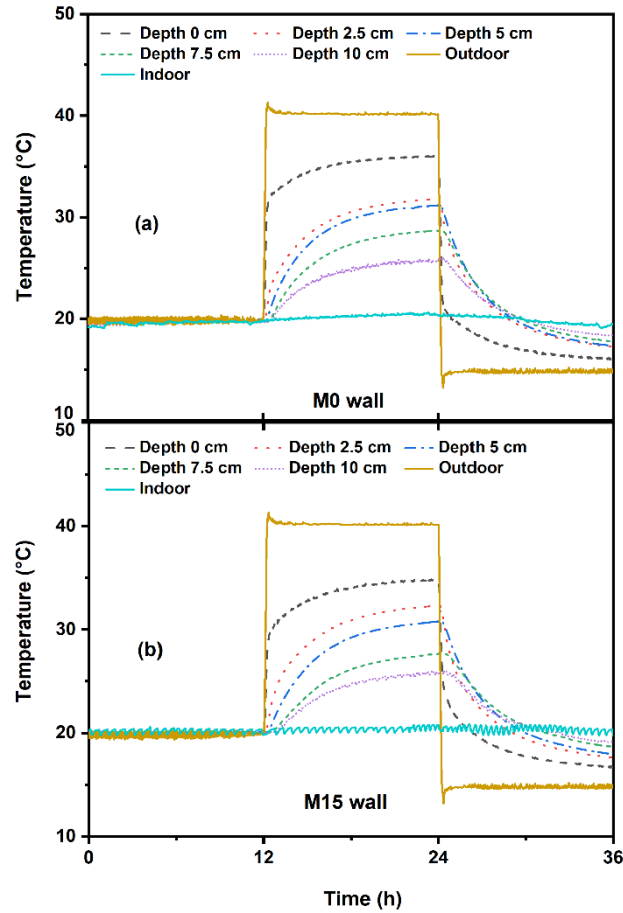
2

Figure 4. M15D enthalpy curve variation calculated using COMSOL.

3 **4. Results**

4 **4.1 Thermal response of the walls under cyclic heating/cooling solicitation**

5 As mentioned in 2.3.3, a stabilization stage was conducted for one week on both walls before
 6 starting the case studies. The first case study is a day/night simulation at controlled hygrome-
 7 try (50% RH) by varying the outdoor temperature between a heating (40°C) and a cooling
 8 (15°C) phase, each lasting 12 hours. The cycles were repeated for more than 7 days to vali-
 9 date the repeatability between the daily cycles. Therefore, the comparison between the ther-
 10 mal responses of the two walls (M0 and M15D) during the heating and cooling phases is pre-
 11 sented in Figures 5 a,b. The evolution of the temperature during one cycle is presented at var-
 12 ious sensor positions during the heating and cooling stages. The trend of the evolution of tem-
 13 perature at various depths in the wall is the same for both walls during the heating and cooling
 14 stages.



1

2

Figure 5. Responses of the walls during 24 hours under temperature solicitation cycles between 40° and 15°C: (a) M0; (b) M15D.

3

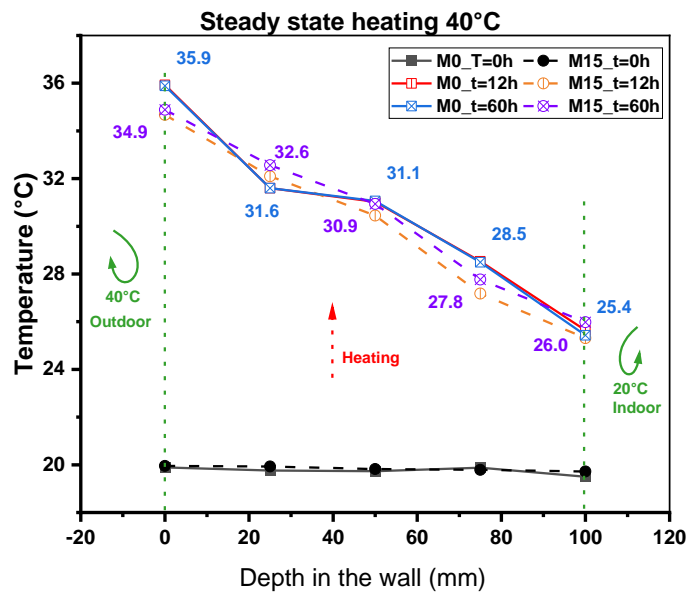
4

5 One noticed the same evolution trends for the temperature during the 24-hour cycle. On the
6 heating stage, the temperature on the outer face of the walls increases rapidly during the first
7 hour and reaches, after 12 hours, a maximum recorded value of 36°C for M0 and 34.8°C for
8 M15D. From the outer face to the inner one, a temperature gradient is observed with decreasing
9 values. A gap is observed in the recorded temperature between the wall M15D and the
10 reference wall. Except at position 25 mm, which can be an error from the sensor position,
11 M15D exhibits a lower temperature than M0 with a gap up to 1°C at 75 mm. The observed
12 reduction in the recorded temperature (~ 1°C) between the two walls may come from the effect
13 of the mPCMs in the wall M15D. The increase in temperature over the melting point of
14 PCM (28 °C) may be stored by the PCM core for phase change to a liquid state. It can reduce
15 the temperature increase's kinetics and induce a small delay in the temperature increase in
16 each position between M15D and M0. On the inner face, the indoor temperature is 20°C and
17 is above the melting point of the PCM, which does not allow the PCM to be activated. The
18 recorded temperature is almost the same for both walls on the inner face.

1 In the cooling phase, when outdoor temperature rapidly decreases from 40°C to 15°C, the
 2 outer face of the wall cools down rapidly. A delayed is observed within the thickness of the
 3 wall with the reverse effect in the temperature gradient. On the outer face (position 0 mm), the
 4 maximum recorded temperature is 16°C for M0 and 17°C for M15D. Here again, the reduc-
 5 tion of ~ 1°C is observed on the PCM wall. Within the thickness of the wall at 24h, the tem-
 6 perature increases nearer the indoor environment (20°C) with recorded value at position 100
 7 mm of 18°C for M0 and 19°C for M15D. One can observe a higher temperature for M15D
 8 than M0 with the gap of about ~ 1°C for sensor positions. On the inner face the temperature is
 9 almost the same for both walls as the PCM are not activated. But when the outdoor tempera-
 10 ture drops below the phase change range, a reverse effect may happen as the PCM started so-
 11 lidification process and the core release the stored energy.

12 4.2 Thermal response of the walls under steady-state heating at 40°C

13 After the cyclic solicitation, the stabilization stage (20°C, 50% RH) is run again before the
 14 second thermal case study. The second case consists in an increase in temperature from 20 to
 15 40°C with a continuous heating at 40°C until steady state. **Figure 6** presents the comparison
 16 of the evolution of the temperature during time variation at various sensors positions of the
 17 two walls.



18

19 **Figure 6.** Comparison between M0 and M15D for a steady-state regime at 40°C

20 The evolution trend of temperature is similar as the one during heating stage of cycling solici-
 21 tation. One can notice that the temperature rapidly increases during the early hours and almost
 22 reaches the maximum value after 12 hours. This result confirms that the highest temperature
 23 is reached during the heating stage of day/night solicitation after 12 hours. For the reference

1 mortar wall M0, the steady state is reached from 12 hours and the recorded temperatures re-
2 mains constant even after long exposure (values at $t = 12\text{h} \cong \text{values at } t = 60\text{h}$). A maximum
3 recorded value of $36\text{ }^\circ\text{C}$ is obtained for the reference wall against $35\text{ }^\circ\text{C}$ for M15D on the out-
4 er face. A temperature gradient is observed from the outdoor face to the indoor across the
5 thickness of the wall.

6 For the wall M15D, there is a small delay between the temperature recorded at 12h and the
7 maximum value at steady state. The same gap of reduction is observed on the temperature
8 within the thickness of the wall. This effect is due to the activation of the PCM as the temper-
9 ature increases over the melting point ($29\text{ }^\circ\text{C}$), the PCM core store the energy and become
10 liquid, delaying the kinetics of the evolution of the temperature. The indoor temperature is
11 constant at $20\text{ }^\circ\text{C}$ and lower than the PCM melting point which doesn't allow the PCM to be
12 activated. The same temperature is almost recorded on the inner face (position 100 mm) with
13 a value $26\text{ }^\circ\text{C}$.

14 Considering all the presented results, the addition of Phase Change Materials (PCMs) has
15 proven effective in mitigating temperature variations in the wall with induce a delay in the
16 kinetic evolution of temperature. Interestingly, more significant effect was anticipated regard-
17 ing the thermophysical properties of the two materials, notably the thermal conductivity, with
18 values of $2.32\text{ W}\cdot\text{m}^{-1}\cdot\text{K}^{-1}$ for M0 and $0.66\text{ W}\cdot\text{m}^{-1}\cdot\text{K}^{-1}$ for M15D at $20\text{ }^\circ\text{C}$. It is worth not-
19 ing that besides boundary conditions, there are other possible phenomena that reduce the ef-
20 fect of the thermal response of the PCM wall.

21 **4.3 Numerical study of building under real climatic conditions**

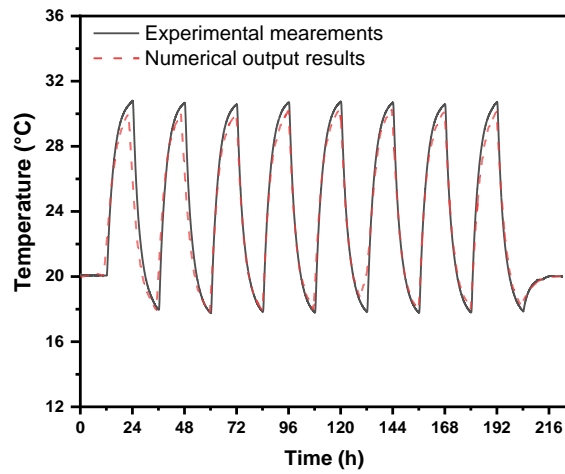
22 The indoor conditions (temperature and energy consumption) seem to be one of the most cru-
23 cial variables to consider when assessing the envelope building performance. High tempera-
24 ture oscillations increase overheating, which is the discomfort felt by building inhabitants be-
25 cause of heat accumulation. Health problems may occur from overheating, especially in the
26 elderly and small children. Therefore, the purpose of this part is to investigate how incorporat-
27 ing bio-based PCM to mortar affects the building's thermal inertia and energy consumption.

28 *4.3.1 Model validation*

29 In this part, EnergyPlus and COMSOL Multiphysics PCM models were validated by compar-
30 ing simulation outcomes with the results of experiments obtained in section 4.1. The heat-
31 ing/cooling test was modeled using both software for the M15D and the simulated tempera-
32 ture was compared with the experimental data.

33 The overview of the experimental and numerical data which use enthalpy model implemented
34 on COMSOL for a thickness of 5 cm of the wall is shown in **Figure 7**. The numerical output
35 results appear to be in good agreement with the experimental data. We notice only a $0.5\text{ }^\circ\text{C}$
36 difference between experimental and numerical data, which can be explained by the sensor
37 accuracy used in the experiments. These findings demonstrate that the model provides accu-

1 rate results and it takes into account the phase shift of PCM particles, especially when the wall
2 temperature is around 29°C, which falls within the temperature range for PCM fusion.



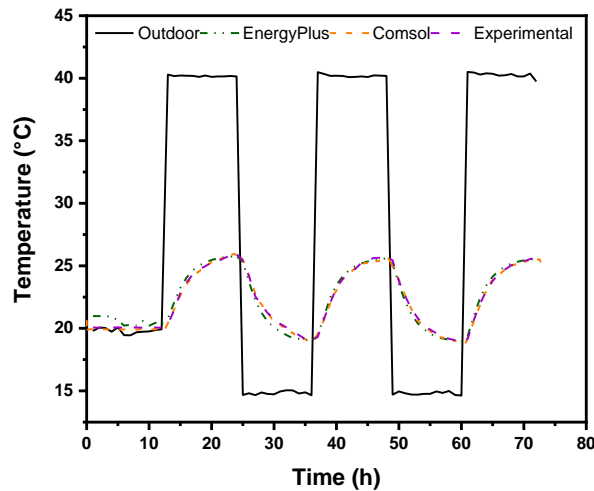
3

4 **Figure 7.** Validation of numerical models using the heating/cooling test at the middle of bio-
5 based PCM wall (5cm)

6 **Figure 8** illustrates a comparison between the experimental measurements and the numerical
7 models for a wall thickness of 10 cm. This thickness was chosen because in EnergyPlus, the
8 numerical simulation enables the prediction of temperature variations solely at the internal
9 and external surfaces. It can be observed that the numerical temperature output closely match-
10 es the experimental data except for the initial hours, where a slight lag is evident. This lag
11 primarily arises from the initialization conditions, including the initial temperature and en-
12 thalpy, employed to initiate the simulation tools.

13 Furthermore, the temperature obtained using COMSOL-Multiphysics closely matches the
14 experimental data, showing nearly the same results. However, a slight difference of approxi-
15 mately 0.5°C is noticed when using EnergyPlus. This difference falls well within the experi-
16 mental error range, indicating that the models are suitable for analyzing the thermal behavior
17 of M15D at the building scale, and the numerical results are considered accurate.

18 Overall, the validation process confirms that both EnergyPlus and COMSOL-Multiphysics
19 models provide reliable results and are appropriate for studying the thermal performance of
20 M15D in building-scale applications.



1

2

Figure 8. Validation of numerical models using the heating/cooling test.

3

Indeed, the PCM model integrated into the EnergyPlus program has been subject to validation in various research studies [33]. For instance, *Salih* et al. [34] found that EnergyPlus simulation results showed good agreement with the numerical work conducted by Alam et al. [35] when a 0.5 cm thick PCM layer was inserted into the ceiling between the plasterboard and the insulation layer. This validation further supports the accuracy of the PCM algorithm.

7

8

Another successful validation of the PCM algorithm was reported by Zhuang et al. [36], who studied two different envelopes with mPCMs: envelope "A" with one layer of PCM and envelope "B" with two layers of PCM. The study showed that the largest relative error in temperature was 12.41% for envelope "A," and the smallest was 0.71%. For envelope "B," the largest relative difference was 8.33%, and the smallest was 0.33%. The study concluded that using the appropriate real weather data and thermal characteristics of the material are crucial factors in reducing differences between simulation and experimental results.

14

15

Furthermore, the PCM algorithm has been validated by Campbell et al. [37] and Chan et al. [38] using experimental data published by Kuznik et al. [39]. In both validation studies, the indoor air temperature predicted by the PCM algorithm in EnergyPlus was found to be in good agreement with the experimental results. These validation studies demonstrate the reliability and accuracy of the PCM algorithm integrated into EnergyPlus, providing confidence in its use for analyzing the thermal behavior of PCM-incorporated building envelopes.

20

21

4.4 Comparison of the thermal behavior of M15D and M0 buildings

22

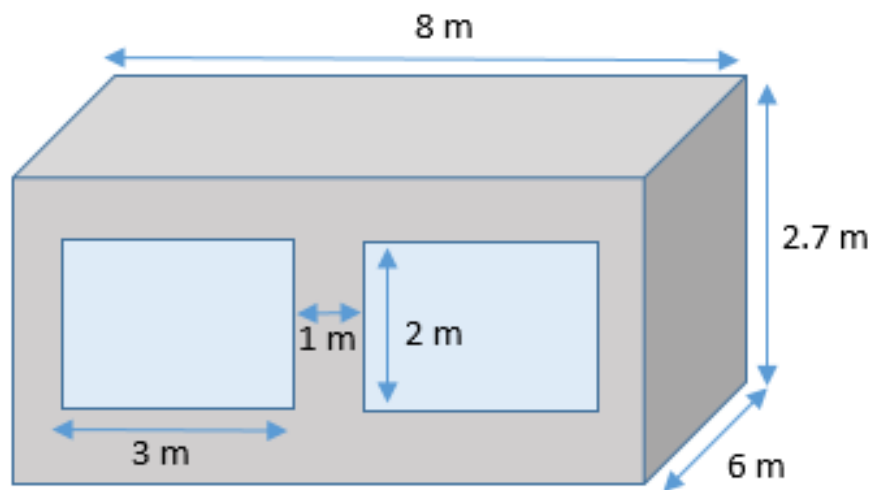
To evaluate the effectiveness of Bio-based Phase Change Materials (PCM) in building envelopes, we conduct in this section a numerical comparison of the thermal performances and energy consumption between both formulation M15D and M0 at the building scale. For this investigation, we selected a simple model of a room representing a typical building known as

25

1 the "BESTEST building," as depicted in **Figure 9**. This building is referenced within the
2 framework of the International Energy Agency (IEA) . The room is a closed space with a vol-
3 ume of 129.6 m^3 ($6 \times 8 \times 2.7 \text{ m}^3$) and features 20 cm-thick external walls. The south facade of
4 the room includes two double-glazed, identical windows.

5 To conduct the comparison, we examine three different climates: a Mediterranean climate
6 represented by Algiers, North of Algeria, a hot and dry climate represented by Ouargla, South
7 of Algeria, and a degraded oceanic climate represented by Paris, France, which implies rela-
8 tively cold winters and relatively hot summers.

9 This study is divided into two parts: the first part involves considering the buildings as pas-
10 sive, meaning no heating or air conditioning is applied. In contrast, the second part involves
11 considering the buildings as air-conditioned to investigate the impact of integrating PCM on
12 energy consumption. To facilitate this analysis, a thermal regulation system has been pro-
13 grammed with set-point temperatures of 20°C for heating and 24°C for cooling.



14

15 **Figure 9.** Geometry of the building model.

16 Indeed, studying the implementation of passive strategies, such as "free-floating" systems, is
17 crucial as it enables the assessment of thermal comfort. Additionally, it facilitates the optimal
18 design of buildings from both architectural and technical perspectives. By exploring passive
19 strategies, it becomes possible to enhance internal thermal conditions, leading to a reduction
20 in the size and energy demands of air conditioning systems. Therefore, in this section, we
21 compare the thermal behavior and inertia of buildings constructed using M15D and M0 mate-
22 rials.

23 To achieve this goal, we employed the enthalpy model to simulate the M15D building, while
24 a basic heat conduction transfer model was utilized for the simulation of the M0 building. Us-
25 ing these simulation approaches, we analyzed the hourly temperature fluctuations for four

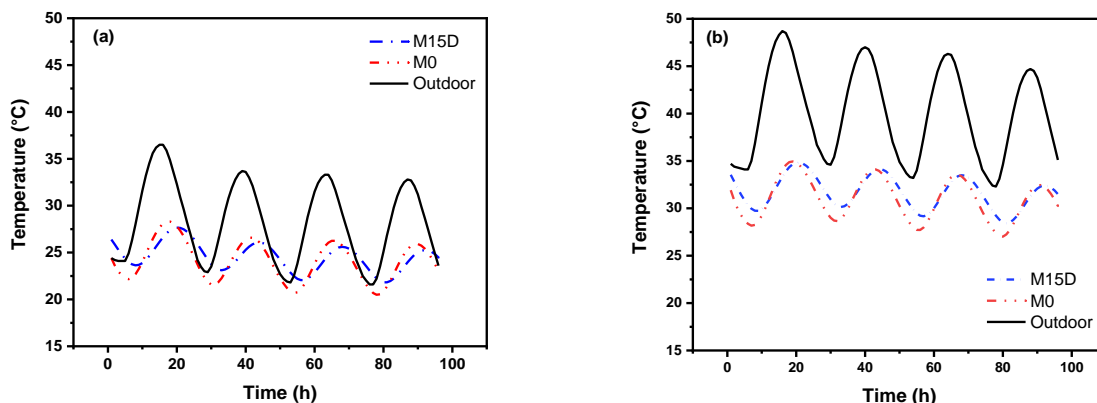
1 representative days during summer conditions, specifically from July 21st to July 24th, in the
2 Mediterranean's hot-dry climate and a degraded oceanic climate. The results of these simula-
3 tions are presented in **Figure 10** (a, b, and c).

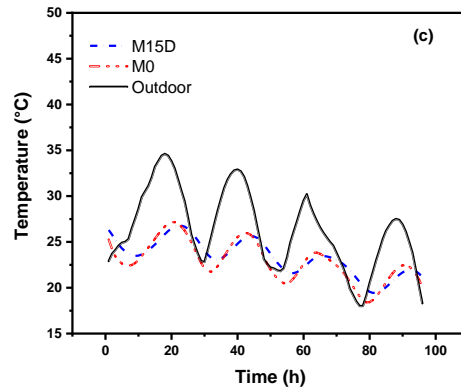
4 In both Mediterranean and degraded oceanic climates, the incorporation of bio-based PCM
5 leads to a decrease in wall temperature during the morning and less efficient heat dissipation
6 during the night, as compared to conventional concrete walls. The results indicate that when
7 the zone temperature reaches the melting range (25-28°C), the bio-based PCM undergoes a
8 phase change, absorbing energy as latent heat, thereby preventing a rapid increase in indoor
9 air temperature. Conversely, when the outdoor temperature drops below 28°C, the PCM initi-
10 ates the solidification process, releasing the stored heat and raising the zone temperature
11 above the reference case.

12 Moreover, it is observed that M15D significantly helps to dampen the periodic temperature
13 variations in comparison to conventional concrete (M0). The damping rate for M15D is esti-
14 mated to be around 34% in the Mediterranean climate, whereas it is approximately 48% for
15 M0. Additionally, the integration of M15D leads to a delay of temperature peaks by approxi-
16 mately 5 hours, whereas M0 only delays the temperature peak by about 2 hours (see Table 3).

17 We also notice that M15D has a greater ability to dampen periodic temperature variations
18 compared to conventional concrete (M0) in the degraded oceanic climate. The damping rate is
19 estimated at 34% for M15D and 48% for M0. Additionally, M15D exhibits a remarkable abil-
20 ity to delay temperature peaks by 5 hours, while M0 only achieves a delay of around 2 hours
21 (Table 3). These results clearly indicate that M15D possesses significant thermal inertia ow-
22 ing to its thermal storage capacity and low thermal diffusivity, setting it apart from M0.

23 These observations hold true even in mild climates, as the melting temperature of the bio-
24 based PCM lies within the range of external temperature variations.





1 **Figure 10.** Simulated indoor temperature of the M15D and AAC M0 buildings: (a) Mediter-
 2 ranean climate and (b) hot-dry climate (c) degraded oceanic climate.

3 In the hot and dry climate (**Figure 10.b**), the findings indeed indicate that the temperature
 4 profile obtained with M15D is almost the same to the one obtained without the PCM (M0).
 5 The outdoor temperature in this climate exceeds the melting point of the bio-based PCM, re-
 6 sulting in the PCM remaining in a liquid state throughout the day.

7 Therefore, the integration of our bio-based PCM with (29°C of melting temperature) is not
 8 advantageous in hot-dry climates under passive conditions. The combination of high outdoor
 9 air temperatures and intense solar radiation during the day leads to the quick melting of the
 10 PCM. Moreover, without a cooling or ventilation system to expedite the solidification pro-
 11 cess, the use of PCM becomes unfavorable in such situations.

12

13

1

Table 3. Damping rate ξ (%) and phase shift (h).

	Mediterranean climate		Hot-dry climate		Degraded oceanic climate	
	M0	M15D	M0	M15D	M0	M15D
ξ (%)	48	34	42	40	41	27
η (h)	2	5	2	3	2	5

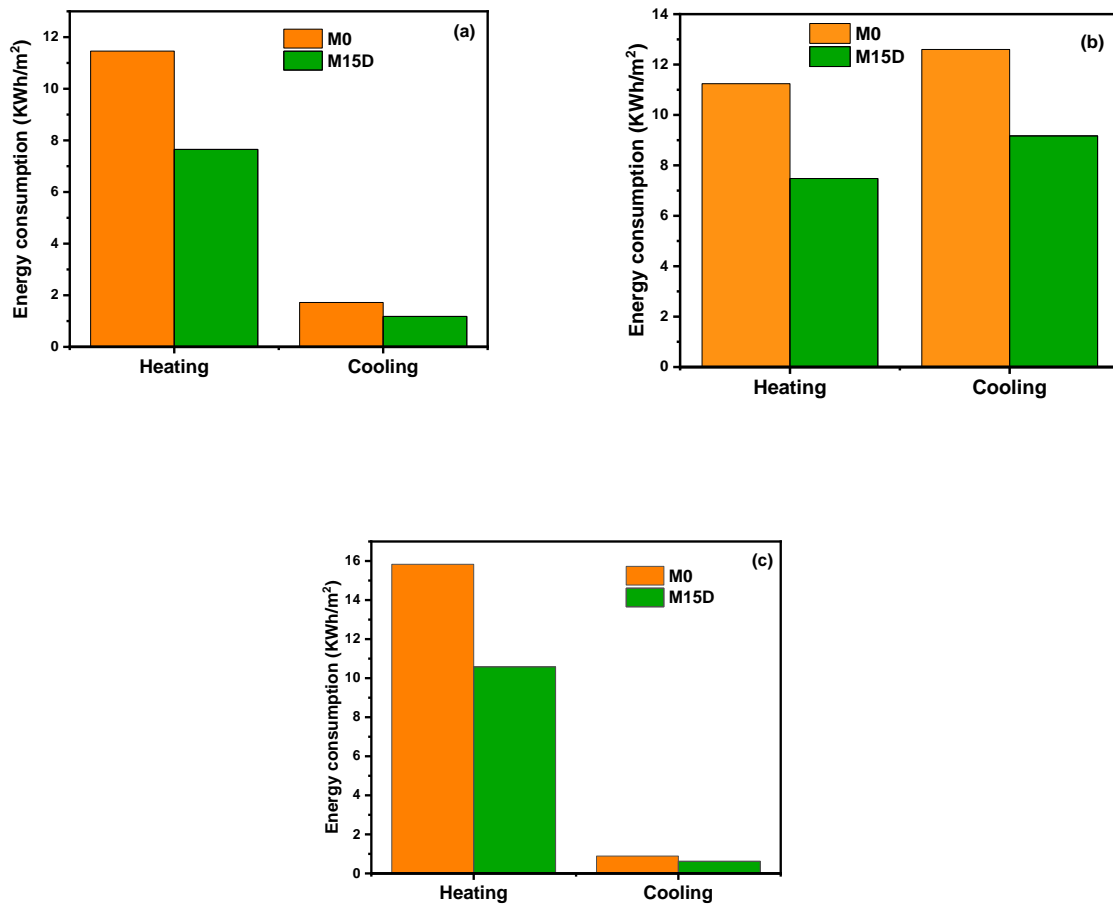
2 Most of the time, the primary advantage of using PCM is to achieve a setback of temperature
3 and reduce peak energy demand. In this section, we examine the energy consumption of
4 buildings constructed with M15D and M0 during both winter and summer periods, consider-
5 ing three different climatic regions (Mediterranean, hot-dry climate, and degraded oceanic
6 climate). The energy consumption for both materials over four representative days in winter
7 and summer is depicted in **Figure 11**.

8 The results clearly show that the integration of bio-based PCM has a positive impact on re-
9 ducing energy consumption across all scenarios. For instance, during winter, M15D allows for
10 a heating energy saving of 33% in both climates, while the saving in cooling energy amounts
11 to approximately 31% in the Mediterranean climate and 27% in the hot-dry climate. However,
12 the energy-saving potential varies significantly depending on the external environmental con-
13 ditions surrounding the building, especially during the summer period.

14 The simulation results reveal several key insights. In hot-dry areas characterized by extreme
15 heat during the summer period, the energy demand for cooling is significantly higher com-
16 pared to Mediterranean or degraded oceanic climate zones. However, due to the wide range of
17 daytime temperatures in these hot-dry regions, there is not enough temperature difference be-
18 tween day and night to facilitate or sustain solidification of the PCM. As a result, the impact
19 on energy savings from PCM integration is limited in such cases.

20 Conversely, during the winter, the results demonstrate an interesting contribution of PCM
21 integration to heating energy savings in buildings across all three climate types. For both
22 Mediterranean and degraded oceanic climates, even though the external temperature is lower
23 than the melting range of M15D, substantial heating energy savings are achieved, highlighting
24 the excellent thermal properties of M15D, including its thermal conductivity and diffusivity.

25 Furthermore, in the hot-dry climate, where the outdoor temperature remains within the melt-
26 ing temperature range of the PCM, there is a maximum benefit from the heat charge/discharge
27 processes in M15D, leading to notable heating energy savings.



1 **Figure 11.** Energy consumption for M15D and for M0 buildings: (a) Mediterranean climate
 2 and (b) hot-dry climate (c) degraded oceanic climate.

3 Table 4. Energy saving using bio-based PCM.

	Saving (%)	
	Heating	Cooling
Mediterranean climate	33	31
Hot and dry climate	33	27
Mild climate	33	29

4

5 5. Conclusion

6 This study investigated the thermal responses of two walls: a reference mortar wall and one
 7 with bio-based microencapsulated phase change materials (PCM). The bi-climatic testing set-
 8 up simulated indoor and outdoor conditions, highlighting the PCM's positive influence on
 9 cement composite thermal performance.

1 Key findings from our research are summarized in the following.

2 During day/night cycles, both walls showed similar temperature trends, but PCM inclusion
3 introduced a controlled damping effect, absorbing and releasing heat during melting and so-
4 lidification.

5 EnergyPlus simulations conducted at the building scale consistently demonstrated notable
6 effects of PCMs on temperature variation and damping rates within model cells. The im-
7 provement in thermal performance was notably impactful in regions marked by substantial
8 daily temperature fluctuations, such as those found in Mediterranean and Degraded oceanic
9 climates. Reduced effectiveness was observed in extremely hot and dry climates, highlighting
10 limitations posed by the swift melting of PCMs in the absence of suitable cooling strategies.

11 Overall, the utilization of bio-based PCMs demonstrates advantages in optimizing building
12 envelopes for enhanced energy efficiency. Significant energy savings and diminished peak
13 demand were evident, particularly during winter seasons, even in climates where seasonal
14 temperatures fall below the melting range of the PCMs.

15 The strategic application of bio-based PCM shows potential for promoting energy sustainabil-
16 ity in construction, contingent on climate conditions. Challenges exist in hot-dry climates,
17 requiring careful consideration of cooling and ventilation strategies.

18 Future research should focus on long-term durability and cost-effectiveness of bio-based PCM
19 integration, exploring tailored applications for specific climates, optimizing PCM composi-
20 tions, and investigating compatibility with other construction materials.

21 In conclusion, this comprehensive study underscores the promising role of bio-based PCM in
22 enhancing energy efficiency, particularly in regions with favorable climatic conditions. As
23 construction trends toward sustainability, the strategic use of PCM offers a tangible solution
24 to address both energy demands and thermal comfort in buildings.

25

26 **Funding:** This research received financial support from the Labex MMCD (Multi-Scale
27 Modelling & Experimentation of Materials for Sustainable Construction), through ANR In-
28 vestments for the Future (program ANR-11-LABX-022-01).

29 **Acknowledgements:** The authors would like to acknowledge Vicat Company for providing
30 the OPC and Alpenat cements used in the experimental part of the study.

31 **Conflicts of interest:** The authors declare no conflict of interest.

1 References

- 2 [1] Yüksek I, Karadayi TT. Energy-efficient building design in the context of building life cycle. *Energy efficient buildings*.
3 2017;10:93-123.
- 4 [2] Cdb P. *Global Status Report for Buildings and Construction*. 2022. 2022.
- 5 [3] Sedillot B, Glorieux-Freminet A. France's energy balance in 2021-provisional data. April 2022. 2022.
- 6 [4] Chel A, Kaushik G. Renewable energy technologies for sustainable development of energy efficient building. *Alexandria*
7 *engineering journal*. 2018;57:655-69.
- 8 [5] Amziane S, Sonebi M. Overview on biobased building material made with plant aggregate. *RILEM Technical Letters*.
9 2016;1:31-8.
- 10 [6] Kalnæs SE, Jelle BP. Phase change materials and products for building applications: A state-of-the-art review and future
11 research opportunities. *Energy and Buildings*. 2015;94:150-76.
- 12 [7] Li C, Wen X, Cai W, Yu H, Liu D. Phase change material for passive cooling in building envelopes: A comprehensive
13 review. *Journal of Building Engineering*. 2023;65:105763.
- 14 [8] Voller V, Shadabi L. Enthalpy methods for tracking a phase change boundary in two dimensions. *International*
15 *communications in heat and mass transfer*. 1984;11:239-49.
- 16 [9] Giro-Paloma J, Martínez M, Cabeza LF, Fernández AI. Types, methods, techniques, and applications for
17 microencapsulated phase change materials (MPCM): A review. *Renewable and Sustainable Energy Reviews*. 2016;53:1059-
18 75.
- 19 [10] Li Q, Ju Z, Wang Z, Ma L, Jiang W, Li D, et al. Thermal performance and economy of PCM foamed cement walls for
20 buildings in different climate zones. *Energy and Buildings*. 2022;277:112470.
- 21 [11] Raj VAA, Velraj R. Review on free cooling of buildings using phase change materials. *Renewable and Sustainable*
22 *Energy Reviews*. 2010;14:2819-29.
- 23 [12] Sharma A, Tyagi VV, Chen CR, Buddhi D. Review on thermal energy storage with phase change materials and
24 applications. *Renewable and Sustainable Energy Reviews*. 2009;13:318-45.
- 25 [13] Cunha S, Sarcinella A, Aguiar J, Frigione M. Perspective on the Development of Energy Storage Technology Using
26 Phase Change Materials in the Construction Industry: A Review. *Energies*. 2023;16:4806.
- 27 [14] Zhan H, Mahyuddin N, Sulaiman R, Khayatian F. Phase change material (PCM) integrations into buildings in hot
28 climates with simulation access for energy performance and thermal comfort: A review. *Construction and Building Materials*.
29 2023;397:132312.
- 30 [15] Bahrar M, Djamai ZI, Mankibi ME, Larbi AS, Salvia M. Numerical and experimental study on the use of
31 microencapsulated phase change materials (PCMs) in textile reinforced concrete panels for energy storage. *Sustainable cities*
32 *and society*. 2018;41:455-68.
- 33 [16] Al-Absi ZA, Hafizal MIM, Ismail M. Innovative PCM-incorporated foamed concrete panels for walls' exterior cladding:
34 An experimental assessment in real-weather conditions. *Energy and Buildings*. 2023;288:113003.
- 35 [17] Hauer A, Mehling H, Schossig P, Yamaha M, Cabeza L, Martin V, et al. Annex 17: advanced thermal energy storage
36 through phase change materials and chemical reactions-feasibility studies and demonstration projects. *International energy*
37 *agency implementing agreement on energy conservation through energy storage*. 2005.
- 38 [18] Zhang H, Xing F, Cui H-Z, Chen D-Z, Ouyang X, Xu S-Z, et al. A novel phase-change cement composite for thermal
39 energy storage: Fabrication, thermal and mechanical properties. *Applied energy*. 2016;170:130-9.
- 40 [19] Li C, Yu H, Song Y. Experimental investigation of thermal performance of microencapsulated PCM-contained
41 wallboard by two measurement modes. *Energy and Buildings*. 2019;184:34-43.

- 1 [20] Li C, Yu H, Song Y, Liu Z. Novel hybrid microencapsulated phase change materials incorporated wallboard for year-
2 long year energy storage in buildings. *Energy Conversion and Management*. 2019;183:791-802.
- 3 [21] Crawley DB, Hand JW, Kummert M, Griffith BT. Contrasting the capabilities of building energy performance
4 simulation programs. *Building and Environment*. 2008;43:661-73.
- 5 [22] Darkwa K, O'callaghan P. Simulation of phase change drywalls in a passive solar building. *Applied Thermal*
6 *Engineering*. 2006;26:853-8.
- 7 [23] Ibanez M, Lázaro A, Zalba B, Cabeza LF. An approach to the simulation of PCMs in building applications using
8 TRNSYS. *Applied Thermal Engineering*. 2005;25:1796-807.
- 9 [24] Koschenz M, Lehmann B. Development of a thermally activated ceiling panel with PCM for application in lightweight
10 and retrofitted buildings. *Energy and Buildings*. 2004;36:567-78.
- 11 [25] Khalil N, Aouad G, El Cheikh K, Rémond S. Use of calcium sulfoaluminate cements for setting control of 3D-printing
12 mortars. *Construction and Building Materials*. 2017;157:382-91.
- 13 [26] TM C. CrodaTherm™ ME29P: Microencapsulated ambient temperature phase change materi-al. 2018.
- 14 [27] Cabeza LF, Castell A, Barreneche Cd, De Gracia A, Fernández A. Materials used as PCM in thermal energy storage in
15 buildings: A review. *Renewable and Sustainable Energy Reviews*. 2011;15:1675-95.
- 16 [28] Gibout S, Franquet E, Haillet D, Bédécarrats J-P, Dumas J-P. Challenges of the usual graphical methods used to
17 characterize phase change materials by differential scanning calorimetry. *Applied sciences*. 2018;8:66.
- 18 [29] Karthikeyan S, Velraj R. Numerical investigation of packed bed storage unit filled with PCM encapsulated spherical
19 containers—a comparison between various mathematical models. *International Journal of Thermal Sciences*. 2012;60:153-60.
- 20 [30] Verma P, Singal SK. Review of mathematical modeling on latent heat thermal energy storage systems using phase-
21 change material. *Renewable and Sustainable Energy Reviews*. 2008;12:999-1031.
- 22 [31] Gbekou FK, Benzarti K, Boudenne A, Eddhahak A, Duc M. Mechanical and thermophysical properties of cement
23 mortars including bio-based microencapsulated phase change materials. *Construction and Building Materials*.
24 2022;352:129056.
- 25 [32] EnergyPlus. EnergyPlus, Getting Started with EnergyPlus Basic: Concepts Manual Essential Infor-mation you need
26 about Running EnergyPlus. In: Energy USDo, editor. c249759bad2022.
- 27 [33] Tabares-Velasco PC, Christensen C, Bianchi M. Verification and validation of EnergyPlus phase change material model
28 for opaque wall assemblies. *Building and Environment*. 2012;54:186-96.
- 29 [34] Salihi M, El Fiti M, Harmen Y, Chhiti Y, Chebak A, Alaoui FEMh, et al. Evaluation of global energy performance of
30 building walls integrating PCM: Numerical study in semi-arid climate in Morocco. *Case Studies in Construction Materials*.
31 2022;16:e00979.
- 32 [35] Alam M, Jamil H, Sanjayan J, Wilson J. Energy saving potential of phase change materials in major Australian cities.
33 *Energy and Buildings*. 2014;78:192-201.
- 34 [36] Zhuang C-l, Deng A-z, Chen Y, Li S-b, Zhang H-y, Fan G-z. Validation of veracity on simulating the indoor
35 temperature in PCM light weight building by EnergyPlus. *International Conference on Intelligent Computing for Sustainable*
36 *Energy and Environment: Springer*; 2010. p. 486-96.
- 37 [37] Campbell KR, Sailor DJ. Phase change materials as thermal storage for high performance homes. *ASME International*
38 *Mechanical Engineering Congress and Exposition*2011. p. 809-18.
- 39 [38] Chan A. Energy and environmental performance of building façades integrated with phase change material in
40 subtropical Hong Kong. *Energy and Buildings*. 2011;43:2947-55.
- 41 [39] Kuznik F, Virgone J, Roux J-J. Energetic efficiency of room wall containing PCM wallboard: a full-scale experimental
42 investigation. *Energy and Buildings*. 2008;40:148-56.

